

Simultaneous multiple angular displacement estimation precision enhanced by the intramode correlation

Shoukang Chang¹, Wei Ye^{2,*}, Xuan Rao², Huan Zhang³, Liqing Huang¹, Mengmeng Luo⁴, Yuetao Chen¹, and Shaoyan Gao^{1†}

¹MOE Key Laboratory for Nonequilibrium Synthesis and Modulation of Condensed Matter, Shaanxi Province Key Laboratory of Quantum Information and Quantum Optoelectronic Devices, School of Physics, Xi'an Jiaotong University, 710049, People's Republic of China

²School of Information Engineering, Nanchang Hangkong University, Nanchang 330063, China

³School of Physics, Sun Yat-sen University, Guangzhou 510275, China

⁴Department of Physics, Xi'an Jiaotong University City College, Xi'an 710018, China

The angular displacement estimation is one of significant branches of quantum parameter estimation. However, most of the studies have focused on the single-angular displacement estimation, while the multiple angular displacement estimation in ideal and noisy scenarios is still elusive. In this paper, we investigate the simultaneous multiple angular displacement estimation based on an orbital angular momentum (OAM), together with inputting $(d + 1)$ -mode NOON-like states as the probe state. By revealing the role of the intramode correlation of the probe state, this allows us to give a reasonable explanation for the corresponding quantum Cramér-Rao bound (QCRB) behaviors with and without photon losses. Our analyses suggest that the QCRB for the multiple angular displacement estimation is always positively related to the intramode correlation, especially for the multimode entangled squeezed vacuum state showing the best performance compared to another probe state. More importantly, strengthening the robustness of multiple angular-displacement estimation systems can be achieved by increasing the OAM quantum number.

PACS: 03.67.-a, 05.30.-d, 42.50.Dv, 03.65.Wj

I. INTRODUCTION

Quantum parameter estimation provides a feasible way to more accurately estimate physical quantities that can not be measured directly than its classical counterpart [1–4]. As a specific example, in phase-estimated systems, the usage of quantum resources, involving non-classical and entanglement states, can make the phase sensitivity beat the so-called shot-noise limit, even closing to the renowned Heisenberg limit [5–7]. In general, the precision limit of quantum parameter estimation can be visually quantified by means of the quantum Cramér-Rao bound (QCRB), which is not only inversely proportional to the quantum Fisher information (QFI) [2, 8], but also has been extensively studied and used especially in quantum single-(or multi-) phase estimation.

Originally, a conventional model to study the quantum parameter estimation is the phase estimation problem [9]. In particular, taking advantage of optical interferometers, such as a Mach-Zehnder interferometer [10–12] and an SU(1,1) interferometer [13–16], early investigations of phase estimation pay attention to the single-phase estimation since it can be easily realized both theoretically and experimentally [5, 11, 15]. More strikingly, the single-phase estimation with the QCRB in the presence of noisy environments, e.g., photon loss [17–19], phase diffusion [20, 21], and thermal noise [22, 23], can be tackled using the variational method [17, 20] pro-

posed by Escher, greatly promoting the practical applications of quantum metrology [24–26]. On the other hand, extending toward the multiple phase estimation with the QCRB has attracted considerable interest more recently, thereby resulting in the potential applications [27–34], such as quantum-enhanced sensor network [29–32] and optical imaging [33, 34]. Moreover, in order to improve the precision of multiple-phase estimation, multimode NOON (or NOON-like) states [35–39], generalized entangled coherent states [40] and multimode Gaussian states [41] have been considered, even in the presence of noisy environment [42–45]. More interestingly, by using correlated quantum states, the simultaneous estimation performance of multiple phases can show a significant advantage scaling as $O(d)$ with the number of phase shifts d over the optimal individual case [35], but the $O(d)$ advantage would fade away in photon-loss scenarios [45]. Further, in order to find saturable QCRB in multiparameter estimation, the necessary and sufficient conditions for projective measurements to saturate the QFI for multiple phase estimation with pure probe states can be achieved [46].

In addition to the phase-estimated systems, the angular displacement estimation based on an orbital angular momentum (OAM) has been one of important branches of parameter-estimated systems, particularly when the OAM quantum number l that is theoretically unbounded can give rise to the unbounded increase in the estimation precision [47–49]. Although the OAM values as high as 10010 quanta have been proven experimentally [50], this value is not indeed unbounded via the limited aperture of optical systems [47, 50, 51]. As a result, other methods have to be found to improve

*Corresponding author. 71147@nchu.edu.cn

†Corresponding author. gaosy@xjtu.edu.cn

the angular displacement estimation. For instance, to show the increased performance of angular displacement estimation, the usages of entangled photon states [49] and twisted NOON states [47] were taken into account. Apart from the aforementioned methods of generating the probe states, Magañ-Loaiza *et al* presented the quantum-improved sensitive estimation of angular rotations based on a sort of weak-value amplification [52]. More dramatically, in ideal and realistic scenarios, Zhang *et al* suggested a super-resolved angular displacement estimation protocol using a Sagnac interferometer together with parity measurement [53]. Even so, it should be noticed that these studies mentioned above pay attention to the single-angular displacement estimation systems, whereas the multiple angular displacement estimation problem in the ideal and noisy environments has not been studied before. Therefore, in this paper, we shall present the derivation of the QCRB for the multiple angular displacement estimation with and without the photon losses when using the $(d+1)$ -mode NOON-like states [including the multimode NOON state (MNOONS), the multimode entangled coherent state (MECS), the multimode entangled squeezed vacuum state (MESVS) and the multimode entangled squeezed coherent state (MESCS)] as the probe states. Our results find that, the QCRB for the multiple angular displacement estimation in both ideal and photon-loss cases is positively associated with the intramode correlation, especially for the MESVS exhibiting the best performance when comparing to other probe states. More interestingly, the OAM quantum number l can be profitably used for strengthening the robustness of multiple angular displacement estimation systems.

The rest of this paper is arranged as follows. In Sec. 2, we first describe the QCRB for the multiple angular displacement estimation with d independent angular displacements in the ideal scenario, and then focus on the behaviors of the QCRB when given the four specific probe states. In Sec. 3, we consider the effects of photon losses on the multiple angular displacement estimation precision, and also analyze its QCRB with the four probe states under the photon losses. Finally, conclusions are presented in the last section.

II. THE QCRB FOR THE MULTIPLE ANGULAR DISPLACEMENT ESTIMATION IN THE IDEAL SCENARIO

In an ideal case, let us beginning with the description of the QCRB for the simultaneous estimation with d independent angular displacements, whose schematic diagram is shown in Fig. 1. To be more specific, here we first take a balanced $(d+1)$ -mode entangled pure as the probe state, which can be defined as [36]

$$|\Psi\rangle = \check{N} \sum_{m=0}^d |0\rangle_0 |0\rangle_1 |0\rangle_2 \dots |\psi\rangle_m \dots |0\rangle_d, \quad (1)$$

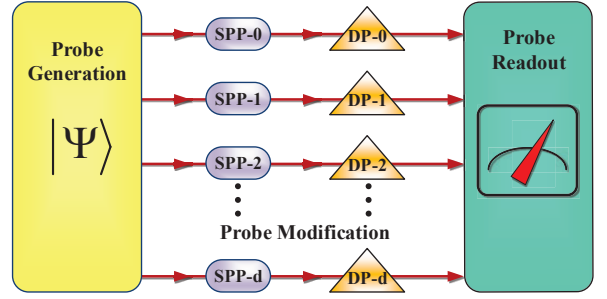


FIG. 1: Schematic diagram of multiple angular displacement estimation with d angular displacements, where a given probe state $|\Psi\rangle$ after passing through spiral phase plate (SPP) and Dove prisms (DP) with the same number $d+1$ can be in read-out.

where $\check{N} = [(1+d)(1+d|\langle\psi|0\rangle|^2)]^{-1/2}$ is the normalization factor. According to Eq. (1), it is obvious that this probe state is a superposition of $d+1$ multimode quantum states with both an arbitrary single-mode quantum state $|\psi\rangle_m$ on the m th mode and a zero photon state on the other modes. It should be mentioned that, when $|\psi\rangle_m$ is respectively the Fock state $|N\rangle_m$, the coherent state $|\alpha\rangle_m$, the squeezed vacuum state $|r_1\rangle_m$ and the squeezed coherent state $|\beta, r_2\rangle_m$, one can obtain the MNOONS $|\Psi_N\rangle$, the MECS $|\Psi_\alpha\rangle$, the MESVS $|\Psi_{r_1}\rangle$ and the MESCS $|\Psi_{\beta, r_2}\rangle$, which will be seen as the probe state to analyze the behaviors of the QCRB in the following sections.

Subsequently, the generated probe state $|\Psi\rangle$ is sent to $d+1$ spiral phase plates (SPPs) which introduce the OAM degree of freedom, and after undergoing the $d+1$ Dove prisms (DPs) to generate d independent angular displacements θ_m to be estimated (here $\theta_0 = 0$ is viewed as the reference beam), the corresponding evolution operator can be expressed as

$$\hat{U}_\theta = \exp\left(i \sum_{m=1}^d 2l\hat{n}_m\theta_m\right), \quad (2)$$

where l is the quanta number of the OAM, $\hat{n}_m = \hat{a}_m^\dagger \hat{a}_m$ and θ_m denote the photon number operator and the angular displacement on mode m , respectively. After the interaction between the probe state and the evolution operator \hat{U}_θ , the resulting state becomes $|\Psi_\theta\rangle = \hat{U}_\theta |\Psi\rangle$, so that the QCRB for the multiple angular displacement estimation in an ideal scenario is given by [35–38]

$$|\delta\theta|^2 \geq |\delta\theta|_{QCRB}^2 = \text{Tr}(F^{-1}), \quad (3)$$

where F^{-1} represents the inverse matrix of the $d \times d$ quantum Fisher information matrix (QFIM). Generally speaking, the QCRB for the multiple angular displacement estimation is not achievable. Nevertheless, for the unitary angular displacement process, i.e., $|\Psi_\theta\rangle =$

$\hat{U}_\theta |\Psi\rangle$, the QCRB of pure quantum states can be saturated if the probe state $|\Psi\rangle$ satisfies [40, 54]

$$\begin{aligned} & \langle \Psi | \left[i(\partial \hat{U}_\theta^\dagger / \partial \theta_j) \hat{U}_\theta, i(\partial \hat{U}_\theta^\dagger / \partial \theta_m) \hat{U}_\theta \right] | \Psi \rangle \\ &= \langle \Psi | [2l \hat{n}_j, 2l \hat{n}_m] | \Psi \rangle \\ &= 0, \quad \forall j, m, \end{aligned} \quad (4)$$

where $\hat{n}_{j,m}$ are the photon number operators on modes j and m . Since both \hat{n}_j and \hat{n}_m are the Hermitian and mutually commuting operators, i.e., $[\hat{n}_j, \hat{n}_m] = 0, \forall j, m$, it is easy for the probe state $|\Psi\rangle$ to find that the saturation condition is always true. Thus, its elements of the QFIM can be given by

$$F_{jm} = 16l^2 \text{Cov}(\hat{n}_j, \hat{n}_m), \quad (5)$$

where $\text{Cov}(\hat{n}_j, \hat{n}_m) = \langle \hat{n}_j \hat{n}_m \rangle - \langle \hat{n}_j \rangle \langle \hat{n}_m \rangle$ is the covariance between the photon number operators \hat{n}_j and \hat{n}_m , and the average $\langle \cdot \rangle$ is taken with respect to the probe state $|\Psi\rangle$. Combining Eqs. (1) and (5), as a result, the QFIM can be calculated as

$$F = 16l^2 \left[\langle \hat{n}_m^2 \rangle I - \langle \hat{n}_m \rangle^2 \tilde{I} \right], \quad (6)$$

where I is the $d \times d$ identity matrix and \tilde{I} represents the matrix with the elements $\tilde{I}_{jm} = 1$, for all j and m . Upon substituting Eqs. (6) into (3), the analytical expression of the QCRB for the multiple angular displacement estimation with the probe state $|\Psi\rangle$ shown in Eq. (1) can be finally derived by

$$\begin{aligned} & |\delta\theta|_{\text{QCRB}}^2 \\ &= \frac{d}{16l^2(\bar{n}_m^2 g_m^{(2)} + \bar{n}_m)} \left(1 + \frac{1}{g_m^{(2)} + \bar{n}_m^{-1} - d} \right), \end{aligned} \quad (7)$$

where $\bar{n}_m = \langle \hat{n}_m \rangle$ denotes the average photon number of the probe state $|\Psi\rangle$ on mode m , and $g_m^{(2)} = \langle \hat{a}_m^\dagger \hat{a}_m^\dagger \hat{a}_m \hat{a}_m \rangle / \bar{n}_m^2$ is the second-order coherence function, represented as an intramode correlation [55]. Generally speaking, the smaller the value of the QCRB, the more precise the parameter estimation. According to Eq. (7), notably, the QCRB is positively correlated with the intramode correlation $g_m^{(2)}$. That is to say, the intramode correlation contributes to the enhancement of multiple angular displacement estimation precision.

To clearly see the behaviors of the QCRB for the multiple angular displacement estimation, here we take four specific probe states into account, including the MNOONS $|\Psi_N\rangle$, the MECS $|\Psi_\alpha\rangle$, the MESVS $|\Psi_{r_1}\rangle$, and the MESCS $|\Psi_{\beta,r_2}\rangle$ as the probe states [see Appendix A for more details]. Without loss of generality, we also assume that both the amplitude α (β) of coherent states and the squeezing parameter r_1 (r_2) are real numbers, so as to achieve the total mean photon numbers \bar{N} for the above four multimode entangled states [see Eq. (10)

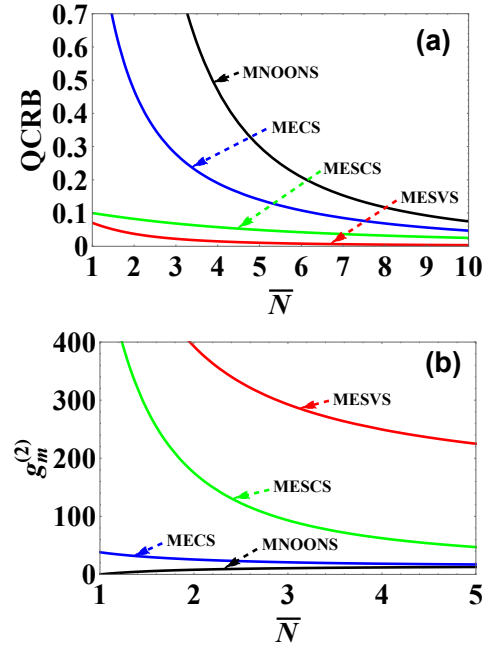


FIG. 2: (Color online) Both (a) the QCRB and (b) the second-order coherence function $g_m^{(2)}$ for the multiple angular displacement estimation as a function of the total mean photon number \bar{N} with several different probe states, i.e., the MNOONS (black line), the MECS (blue line), the MESVS (red line), and the MESCS (green line), at fixed parameters of $l = 2$ and $d = 15$.

in Ref. [36]]. In this case, Fig. 2(a) shows the QCRB for the four multimode entangled states changing with the total mean photon number \bar{N} , when fixed values of $l = 2$ and $d = 15$. It is shown that the value of the QCRB for the given multimode entangled states rapidly decreases with the increase of \bar{N} . Moreover, at the same total mean photon number \bar{N} , the MESVS (red line) shows the lowest QCRB value, followed by the MESCS (green line), the MECS (blue line) and the MNOONS (black line), which means that the usage of the MESVS as the probe state can achieve the highest estimation precision. The reason for this phenomenon is that the intramode correlation of the MESVS is the strongest in comparison to another multimode probe state, as shown in Fig. 2(b). In this sense, it is also demonstrated that the intramode correlation is conducive to effectively improve the multiple angular displacement estimation precision.

On the other hand, we also consider the effects of both the number of independent angular displacements d and the quanta number of the OAM l on the QCRB, as depicted in Fig. 3. It is clearly seen from Fig. 3(a) that when fixed parameters of $l = 2$ and $\bar{N} = 5$, the QCRB for the four probe states increases with the increase of d , meaning that as the number of independent angular displacements d increases, the multiple angular displacement estimation precision becomes worse. This phenomenon results from that the QCRB is passively corre-

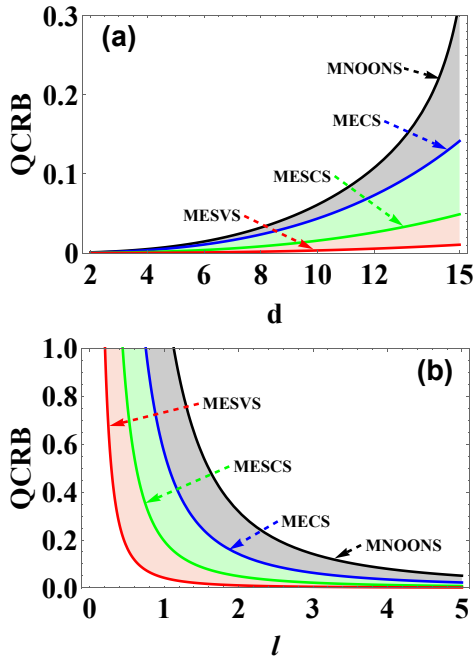


FIG. 3: (Color online) The QCRB for the multiple angular displacement estimation as a function of (a) the independent angular-displacement number d with $l = 2$ and $\bar{N} = 5$, and of (b) the quanta number of the OAM l with $d = 15$ and $\bar{N} = 5$, when given several different probe states, i.e., the MNOONS (black line), the MECS (blue line), the MESCS (green line), and the MESVS (red line).

lated with the number of independent angular displacements d , as given in Eq. (7). Even so, as we can see in Fig. 3(b), at fixed parameters of $d = 15$ and $\bar{N} = 5$, when increasing the quanta number of the OAM l , the QCRB for the four probe states tends to be smaller and smaller. This reflects, to some extent, that increasing l can effectively improve the multiple angular displacement estimation precision. More importantly, it is seen from Fig. 3 that compared to other probe states, the MESVS still maintains the highest estimation precision.

III. THE QCRB FOR THE MULTIPLE ANGULAR

DISPLACEMENT ESTIMATION WITH PHOTON LOSSES

In the real-life scenarios, the inevitable interaction between the probe state system S and its surrounding environment E is always existed, greatly making the parameter-estimated performance worse. In general, there are various interactions, such as photon loss, phase diffusion, and thermal noise. For the sake of simplicity, here we only pay attention to how the photon losses affect the multiple angular displacement estimation precision. In addition, it should be noted that the probe state interacts with the $d+1$ DPs to generate d independent an-

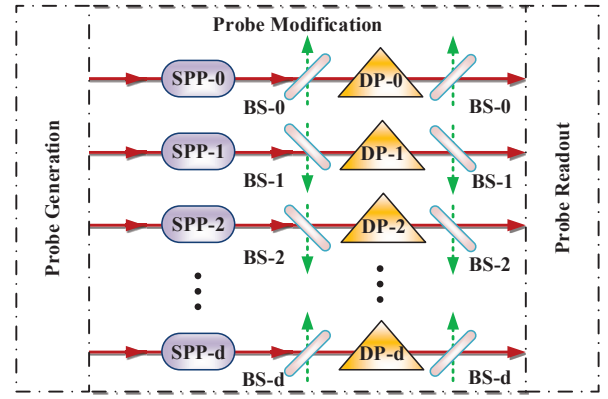


FIG. 4: (Color online) Schematic diagram of multiple angular displacement estimation with d angular displacements under the photon losses occurring at both ends of $d+1$ DPs. Here we use the fictitious beam splitter (BS) with a transmissivity η_m to simulate a photon-loss process

gular displacements θ_m in the photon-loss environment, which would no longer be an unitary evolution. This also leads to that, for the multiple angular displacement estimation with photon losses, the methods used to derive the QCRB given in Eq. (7) can not be directly employed. Fortunately, with the assistance of an variational method, Yue *et al.* derived the general form of the QCRB of multiphase estimation systems in the photon-loss case [45]. By extending that work [45], in this section, we shall utilize the variational method to study the effects of photon losses on the multiple angular displacement estimation precision (see Fig.4), such that a brief review of this variational approach is necessary in the following.

When given an initial $(d+1)$ -mode probe state $|\Psi\rangle_S$ in the probe system S and an initial state $|\vec{0}\rangle_E$ in the photon-loss environment, it is essential to expand the sizes of both the probe system space S and the photon-loss environment space E , thereby resulting in that the probe state $|\Psi\rangle_S$ in the enlarged system-environment space $S+E$ undergoes the unitary evolution $\hat{U}_{S+E}(\theta)$, which can be expressed as [45]

$$\begin{aligned} & |\Psi(\theta)\rangle_{S+E} \\ &= \hat{U}_{S+E}(\theta) |\Psi\rangle_S |\vec{0}\rangle_E \\ &= \sum_k \hat{\Pi}_k(\theta) |\Psi\rangle_S |\vec{k}\rangle_E, \end{aligned} \quad (8)$$

where $\hat{U}_{S+E}(\theta) = \otimes_{m=0}^d \hat{U}_{S+E}^m(\theta_m)$ is the unitary evolution operator, $|\vec{0}\rangle_E = \otimes_{m=0}^d |0\rangle_{E_m}$ is the initial state of environment, $|\vec{k}\rangle_E = \otimes_{m=0}^d |k_m\rangle_{E_m}$ is the orthogonal basis of the environment, and $\hat{\Pi}_k(\theta) = \otimes_{m=0}^d \hat{\Pi}_{k_m}(\theta_m)$ is

the direct product of all kraus operator, defined as

$$\hat{\Pi}_{k_m}(\theta_m) = \sqrt{\frac{(1-\eta_m)^{k_m}}{k_m!}} e^{i2l\theta_m(\hat{n}_m - \delta_m k_m)} \eta_m^{\frac{\hat{n}_m}{2}} \hat{a}_m^{k_m}, \quad (9)$$

with the variational parameters δ_m ($\delta_m = 0$ and -1 are respectively the photon losses occurring before and after the $d+1$ DPs), and η_m quantifying the strength of the photon losses. In practice, such a photon-loss strength can be often regarded as the transmissivity of fictitious beam splitters, as seen in Fig. 4. Among them, $\eta_m = 0$ and 1 respectively indicate the complete-absorption and lossless cases. In this situation, the QCRB for the multiple angular displacement estimation under the photon losses turns out to be [45]

$$|\delta\theta|_{QCRBL}^2 = \max_{\hat{\Pi}_k(\theta)} \text{Tr}[C_Q^{-1}(\theta, \hat{\Pi}_k(\theta))], \quad (10)$$

where $C_Q(\theta, \hat{\Pi}_k(\theta))$ is the QFIM for the enlarged system-environment space $S+E$, and the matrix elements of $C_Q(\theta, \hat{\Pi}_k(\theta))$ are expressed as

$$C_{Q_{jm}}(\theta, \hat{\Pi}_k(\theta)) = 4 \left[\langle \hat{\Lambda}_{jm} \rangle - \langle \hat{\Gamma}_j \rangle \langle \hat{\Gamma}_m \rangle \right], \quad (11)$$

with

$$\hat{\Gamma}_m = i \sum_{k_m} \frac{d\hat{\Pi}_{k_m}^\dagger(\theta_m)}{d\theta_m} \hat{\Pi}_{k_m}(\theta_m),$$

$$\hat{\Lambda}_{jm} = \begin{cases} \sum_{k_m} \frac{d\hat{\Pi}_{k_m}^\dagger(\theta_m)}{d\theta_m} \frac{d\hat{\Pi}_{k_m}(\theta_m)}{d\theta_m}, & j = m \\ \hat{\Gamma}_j \hat{\Gamma}_m, & j \neq m \end{cases}. \quad (12)$$

Upon substituting Eqs. (9) into (12), one can further obtain

$$\hat{\Gamma}_m = 2l\chi_m \hat{n}_m,$$

$$\hat{\Lambda}_{jm} = \begin{cases} 4l^2(\chi_m^2 \hat{n}_m^2 + \gamma_m \hat{n}_m), & j = m \\ \hat{\Gamma}_j \hat{\Gamma}_m, & j \neq m \end{cases}, \quad (13)$$

with $\chi_m = 1 - (1 + \delta_m)(1 - \eta_m)$ and $\gamma_m = \eta_m(1 - \eta_m)(1 + \delta_m)^2$. For the sake of calculation, here we only consider the specific cases of $\eta_m = \eta$ and $\delta_m = \delta$ for any m . Thus, based on Eqs. (11) and (13), one can derive the lower bound of the QCRB for the multiple angular displacement estimation, i.e.,

$$\text{Tr}[C_Q^{-1}] = \frac{(d-1)\check{N}^{-2}}{16l^2\sigma} + \frac{\check{N}^{-2}}{16l^2 \left[\sigma - d\check{N}^2\chi^2 \langle \psi | \hat{n} | \psi \rangle^2 \right]}, \quad (14)$$

where $\sigma = \chi^2 \langle \psi | \hat{n}^2 | \psi \rangle + \gamma \langle \psi | \hat{n} | \psi \rangle$. To further simplify the calculation, we also assume that $d \gg 1$, leading to

that the second term is infinitesimal compared with the first term given in Eq. (14), such that

$$\text{Tr}[C_Q^{-1}] \approx \frac{(d-1)\check{N}^{-2}}{16l^2\sigma}. \quad (15)$$

In order to maximize $\text{Tr}[C_Q^{-1}]$, the optimal value of δ can be easily calculated as

$$\delta_{opt} = \frac{\langle \psi | \hat{n}^2 | \psi \rangle}{(1-\eta) \langle \psi | \hat{n}^2 | \psi \rangle + \eta \langle \psi | \hat{n} | \psi \rangle} - 1. \quad (16)$$

Therefore, substituting Eqs. (16) into (15), one can obtain the explicit expression of the QCRB for the multiple angular displacement estimation in the presence of photon losses, i.e.,

$$|\delta\theta|_{QCRBL}^2 = \frac{d-1}{16l^2\bar{n}_m} \left(\frac{1-\eta}{\eta} + \frac{1}{1+\bar{n}_m g_m^{(2)}} \right). \quad (17)$$

From Eq. (17), it is clear that the QCRB is also positively correlated with the intramode correlation $g_m^{(2)}$ even in the presence of photon losses.

Next, in order to analyze the effects of the photon losses on the QCRB, let us consider the four probe resources, involving the MNOONS $|\Psi_N\rangle$, the MECS $|\Psi_\alpha\rangle$, the MESVS $|\Psi_{r_1}\rangle$, and the MESCS $|\Psi_{\beta, r_2}\rangle$ [One can refer to Appendix B about the expressions of the QCRB for these probe states]. When given the values of $\check{N} = 5$, $d = 15$ and $l = 2$, we plot the QCRB as a function of the photon-loss strength η for the four probe resources, as depicted in Fig. 5(a). As we can see, the value of the QCRB for these probe states increases rapidly with the decrease of η , implying that the accuracy of the multiple angular displacement estimation is greatly affected by the photon losses. In spite of this, the QCRB for the MESVS (red dashed line) still shows the best performance even in the presence of photon losses, followed by the MESCS, the MECS and the MNOONS. Moreover, in order to compare the gap between the ideal and photon-loss cases, at fixed parameters of $\eta = 0.7$, $d = 15$ and $l = 2$, we also show the QCRB changing with the mean photon number \check{N} for the given probe resources, i.e., the MNOONS (black lines), the MECS (blue lines), the MESVS (red lines), and the MESCS (green lines), as pictured in Fig. 5(b). It is clearly seen that, although the QCRB for the MNOONS performs worse than that for other probe states with and without the photon losses, its gap between the ideal and photon-loss cases is the smallest. This means that applying the MNOONS into multiple angular displacement estimation systems is more robust against photon losses than other probe resources at the same conditions. More interestingly, for these probe resources, both the QCRB and the gap with and without the photon losses can be further reduced as the mean photon number \check{N} increases, implying that the increase

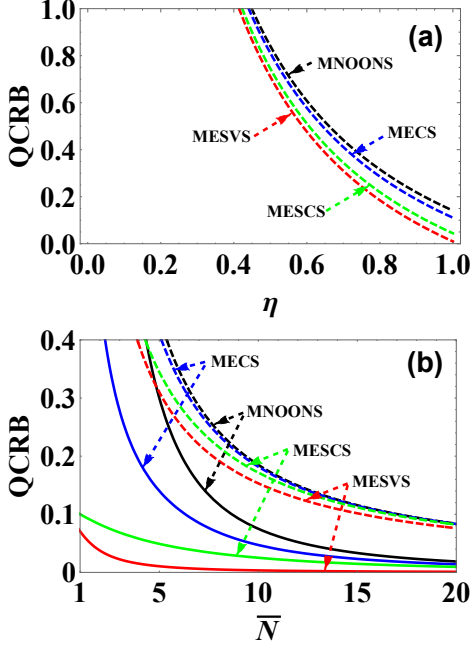


FIG. 5: (Color online) The QCRB for the multiple angular displacement estimation as a function of (a) the photon-loss strength η with $l = 2$, $d = 15$, and $\bar{N} = 5$, and of (b) the mean photon number \bar{N} with $l = 2$, $d = 15$ and $\eta = 0.7$, when inputting the MNOONS (black lines), the MECS (blue lines), the MESVS (red lines), and the MESCS (green lines). The dashed and solid lines correspond to the photon-loss and ideal cases, respectively.

of the mean photon number \bar{N} of probe states is a highly effective way to enhance the multiple angular displacement estimation performance.

On the other hand, we also examine the influences of both d and l on the QCRB under the photon losses when given parameters of $\eta = 0.7$ and $\bar{N} = 5$, as pictured in Fig. 6. Analogous to the ideal cases, for the photon losses as the d (l) increases, the multiple angular displacement estimation precision becomes worse (more precise), and the MESVS still maintains the highest estimation precision even beyond the ideal case of the MNOONS. In addition, we also notice that, when given the same probe state, e.g., the MESVS, as the d (l) increases, the corresponding gap between the ideal and photon-loss scenarios increases (decreases), implying that the decrease of d (or the increase of l) can not only improve the multiple angular displacement estimation precision, but also enhance the robustness against the photon losses. However, for different probe states, such as the MESVS and the MECS shown in Fig. 6(a), their gaps can not be directly visualized and compared. For this reason, to intuitively quantify and visualize the gaps for the four probe states, we give the definition of the robustness against the photon losses, i.e.,

$$R = |\delta\theta|_{QCRB_L}^2 - |\delta\theta|_{QCRB}^2. \quad (18)$$

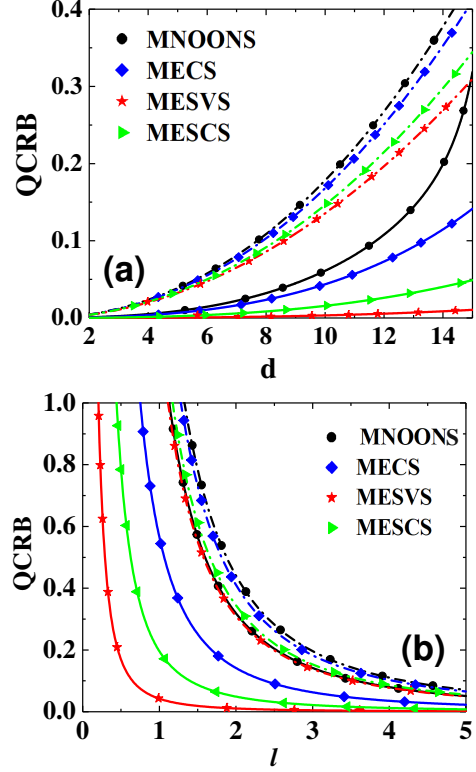


FIG. 6: (Color online) The QCRB for the multiple angular displacement estimation as a function of (a) the number of independent angular displacements d with $\eta = 0.7$, $l = 2$ and $\bar{N} = 5$, and of (b) the quanta number of the OAM l with $\eta = 0.7$, $d = 15$ and $\bar{N} = 5$, when inputting the MNOONS (black lines), the MECS (blue lines), the MESVS (red lines) and the MESCS (green lines). The dashed and solid lines correspond to the photon-loss and ideal cases, respectively.

From Eq. (18), the smaller the value of R , the smaller the gap between $|\delta\theta|_{QCRB_L}^2$ and $|\delta\theta|_{QCRB}^2$, meaning that the robustness against the photon losses is stronger. To see this point, Fig. 7 shows the R changing with d and l for the four probe resources when given parameters of $\eta = 0.7$ and $\bar{N} = 5$. Visually, for the given probe resources, the corresponding robustness R is positively correlated with l and negatively correlated with d . In particular, it is more interesting that the MNOONS presents the best robustness, followed by the MECS, the MESCS, and the MESVS, which is completely opposite to the presentation accuracy of their multiple angular displacement estimations. That is to say, the QCRB for the MNOONS shows the worst performance with and without the photon losses compared to other probe resources, but the usage of the MNOONS in the multiple angular displacement estimation systems has the best robustness. Furthermore, it is worth mentioning that, when comparing to other probe resources, the robustness performance for the MESVS against the photon losses is relatively poor, but can gradually approach the robustness of the

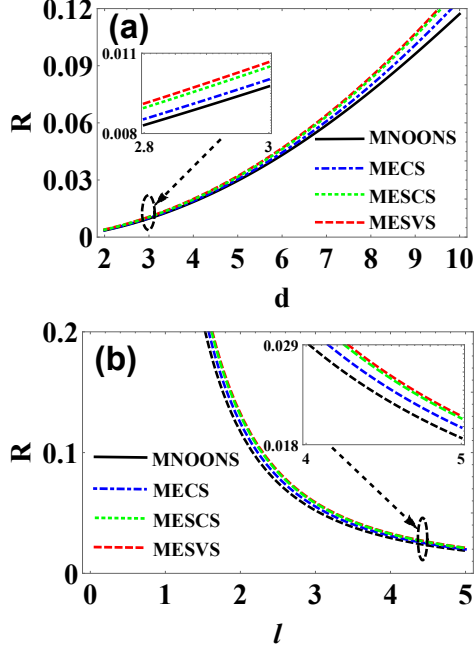


FIG. 7: (Color online) The R for the multiple angular displacement estimation as a function of (a) the number of independent angular displacements d with $\eta = 0.7$, $l = 2$ and $\bar{N} = 5$, and of (b) the quanta number of the OAM l with $\eta = 0.7$, $d = 10$ and $\bar{N} = 5$, when inputting the MNOONS (black solid line), the MECS (blue dot-dashed line), the MESVS (red dashed line) and the MESCS (green dot line).

MNOONS with the increase of l , which also means that the OAM quantum number l is profitably used for enhancing the robustness of multiple angular displacement estimation systems.

IV. CONCLUSIONS

In summary, we have revealed an important factor, i.e., the intramode correlation of the probe state, which affects the multiple angular displacement estimation precision with and without the photon losses. This finding offers a reasonable explanation for the multiple angular displacement estimation performance with $(d + 1)$ -mode NOON-like probe states. The results show that the usage of the MESVS as the probe state is more beneficial for obtaining the highest estimation precision than another multimode probe state, which results from the intramode correlation of the MESVS is the strongest. We have also considered the effects of the photon losses on the multiple angular displacement estimation precision by the means of the variational method. The results suggest that the accuracy of the multiple angular displacement estimation is greatly affected by the photon losses, but the QCRB for the MESVS still shows the best estimation performance when comparing

to the one for another probe state. More interestingly, different from the multiphase estimated systems, we can also regulate and control the quanta number of the OAM l to effectively improve the robustness and precision of multiple angular displacement estimation.

Acknowledgments

We sincerely thank Prof. Yu-Ran Zhang and Heng Fan for helpful discussions. This work was supported by the National Nature Science Foundation of China (Grant Nos. 91536115, 11534008, 62161029); Natural Science Foundation of Shaanxi Province (Grant No. 2016JM1005); Natural Science Foundation of Jiangxi Provincial (Grant No. 20202BABL202002). Wei Ye is supported by both the Natural Science Foundation of Jiangxi Province Youth Fund Project and the Scientific Research Startup Foundation (Grant No. EA202204230) at Nanchang Hangkong University.

Appendix A: The QCRB of four specific multimode entangled state in the deal case

Based on Eq. (7), one can get the

$$\begin{aligned}
 & |\delta\theta|_{QCRB(MNOONS)}^2 \\
 &= \frac{d}{16l^2(\bar{n}_{m(N)}^2 g_{m(N)}^{(2)} + \bar{n}_{m(N)})} \left(1 + \frac{1}{g_{m(N)}^{(2)} + \bar{n}_{m(N)} - d} \right), \\
 & |\delta\theta|_{QCRB(MECS)}^2 \\
 &= \frac{d}{16l^2(\bar{n}_{m(\alpha)}^2 g_{m(\alpha)}^{(2)} + \bar{n}_{m(\alpha)})} \left(1 + \frac{1}{g_{m(\alpha)}^{(2)} + \bar{n}_{m(\alpha)} - d} \right), \\
 & |\delta\theta|_{QCRB(MESVS)}^2 \\
 &= \frac{d}{16l^2(\bar{n}_{m(r_1)}^2 g_{m(r_1)}^{(2)} + \bar{n}_{m(r_1)})} \left(1 + \frac{1}{g_{m(r_1)}^{(2)} + \bar{n}_{m(r_1)} - d} \right), \\
 & |\delta\theta|_{QCRB(MESCS)}^2 = \frac{d}{16l^2(\bar{n}_{m(\beta,r_2)}^2 g_{m(\beta,r_2)}^{(2)} + \bar{n}_{m(\beta,r_2)})} \\
 & \times \left(1 + \frac{1}{g_{m(\beta,r_2)}^{(2)} + \bar{n}_{m(\beta,r_2)} - d} \right), \tag{A1}
 \end{aligned}$$

where we have set

$$\begin{aligned}
\bar{n}_{m(N)} &= \check{N}_N^2 N, \\
g_{m(N)}^{(2)} &= \frac{N-1}{\bar{n}_{m(N)}}, \\
\bar{n}_{m(\alpha)} &= \check{N}_\alpha^2 \alpha^2, \\
g_{m(\alpha)}^{(2)} &= \frac{1}{\check{N}_\alpha^2}, \\
\bar{n}_{m(r_1)} &= \check{N}_{r_1}^2 \sinh^2 r_1, \\
g_{m(r_1)}^{(2)} &= \frac{\check{N}_{r_1}^2 (3 \cosh 2r_1 - 7) \cosh^2 r_1 + 4}{2\bar{n}_{m(r_1)}^2}, \\
\bar{n}_{m(\beta, r_2)} &= \check{N}_{\beta, r_2}^2 (\beta^2 + \sinh^2 r_2), \\
g_{m(\beta, r_2)}^{(2)} &= \frac{\check{N}_{\beta, r_2}^2 (Z_1 + Z_2) + 2}{\bar{n}_{m(\beta, r_2)}^2}, \tag{A2}
\end{aligned}$$

with

$$\begin{aligned}
\check{N}_N &= \frac{1}{\sqrt{1+d}}, \\
\check{N}_\alpha &= \frac{1}{\sqrt{(1+d)(1+de^{-\alpha^2})}}, \\
\check{N}_{r_1} &= \frac{1}{\sqrt{(1+d)(1+d \sec hr_1)}}, \\
\check{N}_{\beta, r_2} &= \frac{1}{\sqrt{(1+d)(1+de^{-\beta^2(1-\tanh r_2)} \sec hr_2)}}, \\
Z_1 &= \beta^2 \sinh(2r_2) + (2\beta^2 - 1) \cosh(2r_2), \\
Z_2 &= \frac{3}{8} \cosh(4r_2) + \beta^4 - 2\beta^2 - \frac{11}{8}. \tag{A3}
\end{aligned}$$

Appendix B: The QCRB of four specific multimode entangled state under the photon losses

According to the Eq. (17), one can obtain

$$\begin{aligned}
|\delta\theta|_{QCRBL(MNOONS)}^2 &= \frac{d-1}{16l^2\bar{n}_{m(N)}} \left(\frac{1-\eta}{\eta} + \frac{1}{1+\bar{n}_{m(N)}g_{m(N)}^{(2)}} \right), \\
|\delta\theta|_{QCRBL(MECS)}^2 &= \frac{d-1}{16l^2\bar{n}_{m(\alpha)}} \left(\frac{1-\eta}{\eta} + \frac{1}{1+\bar{n}_{m(\alpha)}g_{m(\alpha)}^{(2)}} \right), \\
|\delta\theta|_{QCRBL(MESVS)}^2 &= \frac{d-1}{16l^2\bar{n}_{m(r_1)}} \left(\frac{1-\eta}{\eta} + \frac{1}{1+\bar{n}_{m(r_1)}g_{m(r_1)}^{(2)}} \right), \\
|\delta\theta|_{QCRBL(MESCS)}^2 &= \frac{d-1}{16l^2\bar{n}_{m(\beta, r_2)}} \left(\frac{1-\eta}{\eta} + \frac{1}{1+\bar{n}_{m(\beta, r_2)}g_{m(\beta, r_2)}^{(2)}} \right), \tag{A4}
\end{aligned}$$

where $\bar{n}_{m(N)}$, $g_{m(N)}^{(2)}$, $\bar{n}_{m(\alpha)}$, $g_{m(\alpha)}^{(2)}$, $\bar{n}_{m(r_1)}$, $g_{m(r_1)}^{(2)}$, $\bar{n}_{m(\beta, r_2)}$, and $g_{m(\beta, r_2)}^{(2)}$ can be given by Eq. (A2).

-
- [1] J. S. Sidhu, Y. K. Ouyang, E. T. Campbell, and P. Kok, Tight Bounds on the Simultaneous Estimation of Incompatible Parameters, *Phys. Rev. X* 11, 011028 (2021).
- [2] A. Z. Goldberg, L. L. Sánchez-Soto, and H. Ferretti, Intrinsic Sensitivity Limits for Multiparameter Quantum Metrology, *Phys. Rev. Lett.* 127, 110501 (2021).
- [3] P. Horodecki, Ł. Rudnicki, and K. Życzkowski, Five Open Problems in Quantum Information Theory, *PRX Quantum* 3, 010101 (2022).
- [4] S. K. Chang, W. Ye, X. Rao, H. Zhang, L. Q. Huang, M. M. Luo, Y. T. Chen, S. Y. Gao, and L. Y. Hu, Evaluating the quantum Ziv–Zakai bound for phase estimation in noisy environments, *Opt. Express* 30, 24207 (2022).
- [5] P. M. Anisimov, G. M. Raterman, A. Chiruvelli, W. N. Plick, S. D. Huver, H. Lee, and J. P. Dowling, Quantum Metrology with Two-Mode Squeezed Vacuum: Parity Detection Beats the Heisenberg Limit, *Phys. Rev. Lett.* 104, 103602 (2010).
- [6] V. Giovannetti, S. Lloyd, and L. Maccone, Quantum Metrology, *Phys. Rev. Lett.* 96, 010401 (2006).
- [7] X. M. Lu and X. G. Wang, Incorporating Heisenberg’s Uncertainty Principle into Quantum Multiparameter Estimation, *Phys. Rev. Lett.* 126, 120503 (2021).
- [8] S. L. Braunstein, and C. M. Caves, Statistical Distance and the Geometry of Quantum States, *Phys. Rev. Lett.* 72, 3439 (1994).
- [9] W. Górecki, and R. Demkowicz-Dobrzański, Multiple-Phase Quantum Interferometry: Real and Apparent Gains of Measuring All the Phases Simultaneously, *Phys. Rev. Lett.* 128, 040504 (2022).
- [10] B. Yurke, S. L. McCall, and J. R. Klauder, SU(2) and SU(1,1) interferometers, *Phys. Rev. A* 33, 4033 (1986).
- [11] J. Joo, W. J. Munro, and T. P. Spiller, Quantum Metrology with Entangled Coherent States, *Phys. Rev. Lett.* 107, 083601 (2011).
- [12] H. Zhang, W. Ye, C. P. Wei, Y. Xia, S. K. Chang, Z. Y. Liao, and L. Y. Hu, Improved phase sensitivity in a quantum optical interferometer based on multiphoton catalytic two-mode squeezed vacuum states, *Phys. Rev. A* 103, 013705 (2021).
- [13] L. L. Guo, Y. F. Yu, and Z. M. Zhang, Improving the phase sensitivity of an SU(1,1) interferometer with photon-added squeezed vacuum light, *Opt. Express* 26, 29099–29109 (2018).
- [14] G. S. Agarwal, and L. Davidovich, Quantifying quantum amplified metrology via Fisher information, *Phys. Rev.*

- Res. 4, L012014 (2022).
- [15] W. Du, J. Kong, G. Z. Bao, P. Y. Yang, J. Jia, S. Ming, C. H. Yuan, J. F. Chen, Z. Y. Ou, M. W. Mitchell, and W. P. Zhang, SU(2)-in-SU(1,1) Nested Interferometer for High Sensitivity, Loss-Tolerant Quantum Metrology, *Phys. Rev. Lett.* 128, 033601 (2022).
- [16] S. K. Chang, W. Ye, H. Zhang, L. Y. Hu, J. H. Huang, and S. Q. Liu, Improvement of phase sensitivity in an SU(1,1) interferometer via a phase shift induced by a Kerr medium, *Phys. Rev. A* 105, 033704 (2022).
- [17] B. M. Escher, R. L. de Matos Filho, and L. Davidovich, General framework for estimating the ultimate precision limit in noisy quantum-enhanced metrology, *Nat. Phys.* 7, 406–411 (2011).
- [18] A. Monras and M. G. A. Paris, Optimal Quantum Estimation of Loss in Bosonic Channels, *Phys. Rev. Lett.* 98, 160401 (2007).
- [19] H. Zhang, W. Ye, C. P. Wei, C. J. Liu, Z. Y. Liao, and L. Y. Hu, Improving phase estimation using number-conserving operations, *Phys. Rev. A* 103, 052602 (2021).
- [20] B. M. Escher, L. Davidovich, N. Zagury, and R. L. de Matos Filho, Quantum Metrological Limits via a Variational Approach, *Phys. Rev. Lett.* 109, 190404 (2012).
- [21] M. G. Genoni, S. Olivares, and M. G. A. Paris, Optical Phase Estimation in the Presence of Phase Diffusion, *Phys. Rev. Lett.* 106, 153603 (2011).
- [22] C. N. Gagatsos, B. A. Bash, S. Guha, and A. Datta, Bounding the quantum limits of precision for phase estimation with loss and thermal noise, *Phys. Rev. A* 96, 062306 (2017).
- [23] X. Yu, X. Zhao, L. Y. Shen, Y. Y. Shao, J. Liu, and X. G. Wang, Maximal quantum Fisher information for phase estimation without initial parity, *Opt. Express* 26, 16292–16302 (2018).
- [24] C. L. Degen, F. Reinhard, and P. Cappellaro, Quantum sensing, *Rev. Mod. Phys.* 89, 035002 (2017).
- [25] L. Pezzè, A. Smerzi, M. K. Oberthaler, R. Schmied, and P. Treutlein, Quantum metrology with nonclassical states of atomic ensembles, *Rev. Mod. Phys.* 90, 035005 (2018).
- [26] D. Braun, G. Adesso, F. Benatti, R. Floreanini, U. Marzolino, M. W. Mitchell, and S. Pirandola, Quantum-enhanced measurements without entanglement, *Rev. Mod. Phys.* 90, 035006 (2018).
- [27] W. Ye, H. Zhong, Q. Liao, D. Huang, L. Y. Hu, and Y. Guo, Improvement of self-referenced continuous-variable quantum key distribution with quantum photon catalysis, *Opt. Express* 27, 17186 (2019).
- [28] W. Ye, Y. Guo, Y. Xia, H. Zhong, H. Zhang, J. Z. Ding, L. Y. Hu, Discrete modulation continuous-variable quantum key distribution based on quantum catalysis, *Acta Phys. Sin.* 69, 060301 (2020).
- [29] H. Kwon, Y. Lim, L. Jiang, H. Jeong, and C. H. Oh, Quantum Metrological Power of Continuous-Variable Quantum Networks, *Phys. Rev. Lett.* 128, 180503 (2022).
- [30] A. J. Brady, C. Gao, R. Harnik, Z. Liu, Z. S. Zhang, and Q. T. Zhuang, Entangled Sensor-Networks for Dark-Matter Searches, *PRX Quantum* 3, 030333 (2022).
- [31] T. J. Proctor, P. A. Knott, and J. A. Dunningham, Multiparameter Estimation in Networked Quantum Sensors, *Phys. Rev. Lett.* 120, 080501 (2018).
- [32] F. Albarelli, J. F. Friel, and A. Datta, Evaluating the Holevo Cramér-Rao Bound for Multiparameter Quantum Metrology, *Phys. Rev. Lett.* 123, 200503 (2019).
- [33] M. Tsang, R. Nair, and X. M. Lu, Quantum Theory of Superresolution for Two Incoherent Optical Point Sources, *Phys. Rev. X* 6, 031033 (2016).
- [34] R. Nair and M. Tsang, Interferometric superlocalization of two incoherent optical point sources, *Opt. Express* 24, 3684–3701 (2016).
- [35] P. C. Humphreys, M. Barbieri, A. Datta, and I. A. Walmsley, Quantum Enhanced Multiple Phase Estimation, *Phys. Rev. Lett.* 111, 070403 (2013).
- [36] L. Zhang, and K. W. C. Chan, Quantum multiparameter estimation with generalized balanced multimode NOON like states, *Phys. Rev. A* 95, 032321 (2017).
- [37] S. Hong, J. Rehman, Y. S. Kim, Y. W. Cho, S. W. Lee, H. Jung, S. Moon, S. W. Han, and H. T. Lim, Quantum enhanced multiple-phase estimation with multi-mode NOON states, *Nat. Commun.* 12, 5211 (2021).
- [38] Y. Maleki, and M. S. Zubairy, Distributed phase estimation and networked quantum sensors with W-type quantum probes, *Phys. Rev. A* 105, 032428 (2022).
- [39] Y. R. Zhang and H. Fan, Quantum metrological bounds for vector parameters, *Phys. Rev. A* 90, 043818 (2014).
- [40] J. Liu, X. M. Lu, Z. Sun, and X. G. Wang, Quantum multiparameter metrology with generalized entangled coherent state, *J. Phys. A: Math. Theor.* 49, 115302 (2016).
- [41] C. N. Gagatsos, D. Branford, and A. Datta, Gaussian systems for quantum-enhanced multiple phase estimation, *Phys. Rev. A* 94, 042342 (2016).
- [42] F. Albarelli, and R. Demkowicz-Dobrzański, Probe Incompatibility in Multiparameter Noisy Quantum Metrology, *Phys. Rev. X* 12, 011039 (2022).
- [43] M. Szczykulska, T. Baumgratz, and A. Datta, Reaching for the quantum limits in the simultaneous estimation of phase and phase diffusion, *Quantum Sci. Technol.* 2, 044004 (2017).
- [44] F. Albarelli, M. Mazelanik, M. Lipka, A. Streltsov, M. Parniak, and R. Demkowicz-Dobrzański, Quantum Asymmetry and Noisy Multimode Interferometry, *Phys. Rev. Lett.* 128, 240504 (2022).
- [45] J. D. Yue, Y. R. Zhang, and H. Fan, Quantum-enhanced metrology for multiple phase estimation with noise, *Sci. Rep.* 4, 5933 (2014).
- [46] L. Pezzè, M. A. Ciampini, N. Spagnolo, P. C. Humphreys, A. Datta, I. A. Walmsley, M. Barbieri, F. Sciarrino, and A. Smerzi, Optimal Measurements for Simultaneous Quantum Estimation of Multiple Phases, *Phys. Rev. Lett.* 119, 130504 (2017).
- [47] M. Hiekkamäki, F. Bouchard, and R. Fickler, Photonic Angular Superresolution Using Twisted NOON States, *Phys. Rev. Lett.* 127, 263601 (2021).
- [48] V. D'Ambrosio, N. Spagnolo, L. D. Re, S. Slussarenko, Y. Li, L. C. Kwek, L. Marrucci, S. P. Walborn, L. Aolita, and F. Sciarrino, Photonic polarization gears for ultra-sensitive angular measurements, *Nat. Commun.* 4, 2432 (2013).
- [49] A. Kumar Jha, G. S. Agarwal, and R. W. Boyd, Super-sensitive measurement of angular displacements using entangled photons, *Phys. Rev. A* 83, 053829 (2011).
- [50] R. Fickler, G. Campbell, B. Buchler, P. Koy Lam, and A. Zeilinger, Quantum entanglement of angular momentum states with quantum numbers up to 10,010, *Proc. Natl. Acad. Sci. U.S.A.* 113, 13642 (2016).
- [51] M. J. Padgett, F. M. Miatto, M. P. J. Lavery, A. Zeilinger, and R. W. Boyd, Divergence of an orbital-angular momentum-carrying beam upon propagation, *New J. Phys.* 17, 023011 (2015).
- [52] O. S. Magaña-Loaiza, M. Mirhosseini, B. Rodenburg,

- and R. W. Boyd, Amplification of Angular Rotations Using Weak Measurements, *Phys. Rev. Lett.* 112, 200401 (2014).
- [53] J. D. Zhang, Z. J. Zhang, L. Z. Cen, J. Y. Hu, and Y. Zhao, Super-resolved angular displacement estimation based upon a Sagnac interferometer and parity measurement, *Opt. Express* 28, 4320 (2020).
- [54] K. Matsumoto, A new approach to the Cramér-Rao-type bound of the pure-state model, *J. Phys. A: Math. Gen.* 35, 3111 (2002).
- [55] J. Sahota, N. Quesada, and D. F. V. James, Physical resources for optical phase estimation, *Phys. Rev. A* 94, 033817 (2016).